Inorganic Chemistry

Communication

pubs.acs.org/IC

Two Amino-Decorated Metal–Organic Frameworks for Highly Selective and Quantitatively Sensing of Hg^{II} and Cr^{VI} in Aqueous Solution

Lili Wen,*[,†] Xiaofang Zheng,[†] Kangle Lv,[‡] Chenggang Wang,[†] and Xiaoyue Xu[†]

[†]Key Laboratory of Pesticide & Chemical Biology of Ministry of Education, College of Chemistry, Central China Normal University, Wuhan, 430079, P. R. China

[‡]Key Laboratory of Catalysis and Materials Science of the State Ethnic Affairs Commission & Ministry of Education, South-Central University for Nationalities, Wuhan 430074, P. R. China

Supporting Information

ABSTRACT: Two amino-decorated metal–organic frameworks have been constructed, which are the rare examples of MOF-based fluorescent probes targeting environmentally relevant guest species, such as Hg (II) and Cr (VI) ions in aqueous solution, with high selectivity and sensitivity. The possible sensing mechanism is also discussed.

During the past few decades, divalent mercuric (Hg^{2+}) and hexavalent chromium (Cr^{6+}) ions have proven to be two of the most severe environmental nonbiodegradable pollutants because of their increasing utilization in industry and agriculture. Exposure to Hg^{2+}, even at low concentrations, can cause adverse health effects, particularly in the central nervous system,[1] whereas Cr^{6+} is a strong oxidant and very carcinogenic.[2] Several advanced techniques[3] have been developed for detecting and quantifying Hg^{II} and Cr^{VI}, including atomic absorption spectrometry, chromatography, and spectrofluorimetry; however, most of these methods are time-consuming, labor-intensive, and indirect-viewed. Therefore, the fast, facile, visual, and quantitative detection of trace aqueous Hg^{II} or Cr^{VI} still remains a challenge in the field of environmental monitoring and protection. Fluorescence-based probes possess the marked virtues of high sensitivity, selectivity, easy operation, and visualization, making them excellent alternatives for the detection of Hg^{II} and Cr^{VI}.

Recently, luminescent functional metal–organic framework (MOF) materials have attracted a significant amount of attention. The luminescent properties of MOFs are highly dependent on their structures, the coordination environment of the metal centers, the characteristics of the pore surfaces, and their interactions with guest species via coordination bonds, hydrogen-bonding and $\pi-\pi$ interactions, etc. For these reasons, efforts have been made to fabricate luminescent-sensing MOFs.[4] Over the past few decades, diverse luminescent MOFs for sensing cations, anions, small molecules, and vapors have been realized.[5] However, the reported MOF sensors for Hg^{II} and Cr^{VI} are relatively scarce to date.[6]

Considering that the amino substituent can act as an auxochromic group, it may promote charge-transfer interactions in the resulting framework.[7] Herein, we present two MOFs, $[Zn(2\text{-}NH_2bdc)(bibp)]_n$ [**1**; 2-NH_2bdc = 2-amino-1,4-benzenedicarboxylic acid and bibp = 4,4′-bis(imidazol-1-ylmethyl)-biphenyl] and $[Cd(2\text{-}NH_2bdc)(tib)\cdot 4H_2O\cdot 0.5DMA]_n$ [**2**; tib = 1,3,5-tris(1-imidazolyl)benzene and DMA = dimethylacetamide], as highly selective and sensitive fluorescent probes for environmentally relevant contaminants, such as aqueous Hg^{II} and Cr^{VI}. A possible sensing mechanism for these MOFs is also discussed.

In a typical synthesis, the solvothermal reaction of 2-NH_2bdc and auxiliary ligand bibp with $Zn(NO_3)_2\cdot 6H_2O$ in *N*,*N*-dimethylformamide/CH_3OH at 100 °C for 3 days leads to the formation of **1** as colorless block-shaped crystals. Single-crystal X-ray structural analysis revealed that each Zn^{II} center lies in a distorted tetrahedral coordination environment, composed of two O atoms from two 2-NH_2bdc^{2-} moieties and two N atoms from independent bibp linkers in **1** (Figure S1a in the Supporting Information, SI). In compound **1**, the bibp bridges lie in the inversion centers and are coordinated to Zn^{II} ions via trans modes. Each 2-NH_2bdc^{2-} moiety links two Zn^{II} atoms in a monodentate coordination fashion to achieve one-dimensional (1D) chains, which are pillared by bibp ligands to generate a three-dimensional (3D) structure (Figure S1c in the SI). Further topological analysis reveals that **1** adopts a 5-fold interpenetrating architecture belonging to class Ia[8] and is related to a 4-connected dia net with a Schläfli symbol of 6^6 (Figure 1a). Complex **2** can be prepared when the auxiliary ligand is changed from exobidentate bibp to trigonal tib and the metal ion is replaced by $Cd(NO_3)_2\cdot 6H_2O$. The Cd^{II} center sites in pentagonal-bipyramidal coordination geometry are composed of two chelating carboxylate groups from two separate 2-

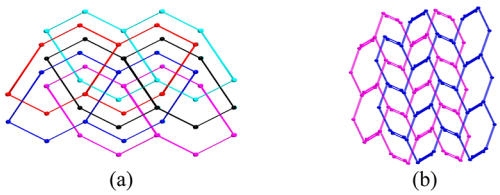

(a) (b)

Figure 1. Schematic views of 5-fold interpenetration of **1** (a) and 2-fold interpenetration of **2** (b).

Received: January 13, 2015
Published: July 13, 2015

DOI: 10.1021/acs.inorgchem.5b00098
Inorg. Chem. 2015, 54, 7133–7135

NH_2bdc^{2-} anions and three N atoms from three distinct tib ligands (Figure S2a in the SI). Each 2-NH_2bdc^{2-} anion is associated with two Cd atoms with both deprotonated carboxylate groups chelating in a bidentate fashion, giving rise to a 1D chain along the *c* direction, which is further bridged by divergent tib ligands to achieve a 3D framework (Figure S2b in the SI). Overall, compound **2** can be represented as a binodal 3,5-connected net with a vertex symbol of $(4^2{\cdot}6^5{\cdot}8^3)(4^2{\cdot}6)$ (Figure 1b). Because of the spacious nature of the single framework, the potential voids can be occupied by another identical 3D net to construct a 2-fold interpenetrating structure belonging to class IIa (Figure S2c in the SI). After interpenetration, the structure still retains 42.2% (2841.5 Å^3 out of the 6734.7 Å^3 unit cell volume) solvent-accessible void volume. Micropore hexagonal windows with areas of 7.0 × 5.3 Å^2 along the *c* axis in **2** are present considering van der Waals distances.

The photoluminescence (PL) spectra of compounds **1** and **2**, as well as free ligand 2-NH_2bdcH_2 in the solid state, were recorded under ambient conditions. Complexes **1** and **2** individually exhibit intense emission peaks at 433 and 422 nm upon excitation at 360 nm, which can be largely attributed to a ligand-centered luminescent process because similar emissions are detected at 551 nm (λ_{ex} = 380 nm) for the free ligand 2-NH_2bdcH_2 (Figure S3a in the SI). In order to examine the potential of **1** for sensing cations, 3 mg of **1** was dispersed in 3 mL of water individually containing 1.0 × 10^{-2} M $M(NO_3)_x$ (M = NH_4^+, Na^+, K^+, Mg^{2+}, Ca^{2+}, Sr^{2+}, Ba^{2+}, Ag^+, Zn^{2+}, Cd^{2+}, and Hg^{2+}) to form cation-incorporated **1** for the detection studies. Interestingly, alkaline and alkaline-earth metal ions, NH_4^+ and Cd^{2+}, do not cause any significant changes in the luminescence intensities. However, different degrees of quenching effects on the luminescence intensities are observed when other ions are involved, with Hg^{2+} causing the most significant changes (Figure 2a), implying that compound **1** can be considered as a promising

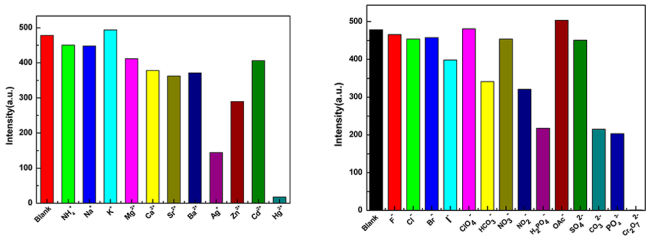

(a) (b)

Figure 2. Effect of various cations (a) and anions (b) at a concentration of 1.0 × 10^{-2} M on the fluorescence intensity of compound **1** at 427 nm.

candidate for selective probing of Hg^{2+}. To assess the sensitivity of **1** toward Hg^{2+} in detail, varying concentrations of Hg^{2+} were introduced into emulsions of **1** dispersed in water and the emissive responses were monitored. The emission intensities clearly decrease gradually with increasing Hg^{2+} concentrations (Figure 3a). The inset of Figure 3a reveals that the strong blue emission of the suspension of **1** can be observed by the naked eye under a usual UV lamp and that its brightness dramatically vanishes with higher concentrations of Hg^{2+}. Quantitatively, the quenching effect can be rationalized by the Stern−Volmer equation: $I_0/I = 1 + K_{SV}[M]$.[9] The values of I_0 and I are the luminescence intensities of the suspension of **1** without and with the addition of Hg^{2+}, respectively. [M] is the molar concentration of Hg^{2+}, and K_{SV} is the Stern−Volmer quenching constant. Figure S4 in the SI shows the Stern−Volmer quenching curve

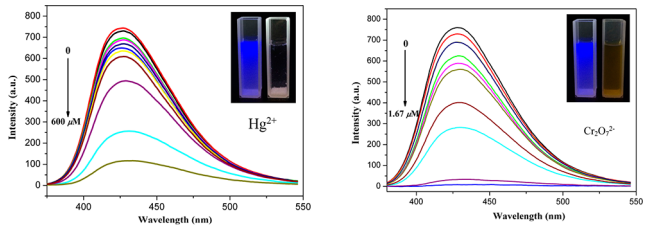

(a) (b)

Figure 3. Fluorescence spectra of **1** in water with increasing amounts of (a) Hg^{2+} (0, 0.12, 0.32, 0.4, 0.6, 2, 4, 16, 120, 200, 400, and 600 μM, respectively) and (b) $Cr_2O_7^{2-}$ (0, 0.001, 0.0033, 0.01, 0.0167, 0.033, 0.0667, 0.133, 0.25, 1, and 1.67 μM, respectively). Inset: photographs taken under UV light (365 nm), showing the fluorescence quenching upon the addition of Hg^{2+} or $Cr_2O_7^{2-}$ to an aqueous emulsion of **1**.

describing I_0/I as a function of the Hg^{2+} concentration in the wide range of 0−600 μM, with a linear fit coefficient of 0.99568, and a K_{sv} value of 4550 M^{-1}.

The possible mechanism for the significant quenching effect of Hg^{2+} is given here. Notably, in **1**, the amino groups of 2-NH_2bdc^{2-} are not coordinated to the Zn^{II} centers and thus extensively decorate the framework as free-standing donors for metal-ion guests. Mercury ions (Hg^{2+}) have a high complexation affinity to N atoms. Therefore, the coordination of Hg^{2+} ions with the pendant amino motif of 2-NH_2bdc^{2-} makes the N atom of −NH_2 prone to changing its hybridization state from sp^2 in **1** to sp^3 in Hg^{2+}-incorporated **1**, causing the amino moiety to deviate from the plane of the benzene ring. These, in turn, may decrease the degree of delocalization in compound **1**, minimizing the energy-transfer efficiency from the π to π* orbital within 2-NH_2bdc^{2-} and thus reducing the overall luminescent intensity. To further investigate the coordination interactions between the amino site and Hg^{2+}, we analyzed compound **1** as well as Hg^{2+}-incorporated **1** using X-ray photoelectron spectroscopy (XPS; Figure 4). The N 1s core-level spectrum of **1** exhibits a broad

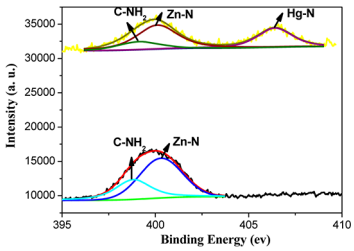

Figure 4. High-resolution XPS spectra for the N 1s region of **1** (lower) and Hg^{2+}-incorporated **1** (upper).

peak at 399.9 eV, which fits well with two peaks at 398.9 and 400.1 eV, respectively assigned to the N atoms from the uncoordinated amino moiety of 2-NH_2bdc^{2-} and coordinated bibp linker. In the presence of Hg^{2+}, a new N 1s peak appears at 406.38 eV, indicating a chelating interaction between the N atom of the amino group in **1** and Hg^{2+}.

In addition, aqueous solutions containing sodium salts of F^-, Cl^-, Br^-, I^-, ClO_4^-, HCO_3^-, NO_3^-, NO_2^-, $H_2PO_4^-$, OAc^-, SO_4^{2-}, CO_3^{2-}, PO_4^{3-}, and $Cr_2O_7^{2-}$ at the same concentration (1.0 × 10^{-2} M) were prepared, and their effects on the fluorescence intensity of **1** were explored. The most interesting feature is that the PL intensities of the different suspensions are strongly dependent on the various anions. The analytes, such as halide ions, ClO_4^-, NO_3^-, OAc^-, and SO_4^{2-}, have negligible

DOI: 10.1021/acs.inorgchem.5b00098
Inorg. Chem. 2015, 54, 7133−7135

effects on the PL intensity, whereas other anions, in particular $Cr_2O_7^{2-}$, significantly decrease the luminescence intensity (Figure 2b). The unusually selective quenching of $Cr_2O_7^{2-}$ prompted us to apply **1** in the detection of trace Cr^{6+} in water. To further evaluate the sensitivity of **1** to Cr^{6+}, we carried out measurements in the presence of varying concentrations of $Cr_2O_7^{2-}$. Our results indicate that the fluorescence intensity of **1** is remarkably suppressed with increasing amounts of $Cr_2O_7^{2-}$ (Figure 3b). The quenching of **1** in the presence of $Cr_2O_7^{2-}$ is most likely due to a decrease in energy transfer between the π and π^* orbitals of 2-NH_2bdc^{2-} because of electron-transfer transitions of $Cr_2O_7^{2-}$.[6] In addition, plotting the quenching efficiency I_0/I versus the Cr^{6+} concentration gives a straight line titration curve, with a correlation coefficient of 0.9957 at low concentrations of 0−0.25 μM. The slope of K_{SV} was calculated to be 6555070 M^{-1}, which is about 565 times larger than the value for functional fluorescent aramids (11600 M^{-1}) used for Cr^{6+} sensing in dimethyl sulfoxide/water and 95 times larger than the value of the fluorescent carbon dot nanosensor (69000 M^{-1}) used for recognition of Cr^{6+} in aqueous solutions. K_{SV} is also superior to the value of Eu^{3+}@MIL-124 (60340 M^{-1}) used for sensing Cr^{6+} in an aqueous environment.[10] The highly selective and sensitive detection of Cr^{6+} in aqueous solutions by compound **1** is remarkable; therefore, it may be considered as a MOF sensor for the quantitative detection of $Cr_2O_7^{2-}$ with the highest sensitivity, an application that has been scarcely reported for MOFs up to now.

The detection limit for Hg^{2+} can reach as low as 4.2×10^{-8} M in aqueous solution for compound **2**, following the 3δ IUPAC criteria, basically satisfying the maximum permitted level of 10 nM Hg^{2+} in drinking water regulated by the U.S. Environmental Protection Agency,[11a] comparable to the sensitivity of nucleic acid functionalized CdSe/ZnS quantum dots for Hg^{2+} (10 nM),[11b] which indicates that **2** is a promising MOF-based sensor for the sensitive and selective detection of Hg^{2+}. However, this value is still lower than that of lanthanide coordination polymer (CP) nanoparticles used for sensing Hg^{2+} (0.2 nM based on a signal-to-noise ratio of 3:1).[6b] Therefore, we are currently exploring the micro/nanostructures of CPs for the probing of analytes, in order to further increase the sensitivity and selectivity of the substrates.

In conclusion, we have successfully synthesized two amino-decorated MOFs for the selective and quantitative detection of Hg^{2+} or Cr^{6+} through fluorescence quenching. In particular, complex **1** represents a MOF sensor that currently possesses the highest reported sensitivity for $Cr_2O_7^{2-}$. The detection limit of compound **2** for Hg^{2+} basically meets the maximum permitted amount in drinking water regulated by the U.S. government. The fluorescence quenching caused by Hg^{2+} can be ascribed to a chelating interaction between the pendant amino motif of 2-NH_2bdc^{2-} and Hg^{2+} in the Hg^{2+}-incorporated compounds, whereas the fluorescence depression caused by Cr^{6+} may be associated with electron-transfer transitions of $Cr_2O_7^{2-}$. This work presents a promising approach for the design of MOF-based sensors for environmentally relevant species, which will probably be useful under more realistic conditions in the future.

■ ASSOCIATED CONTENT

Supporting Information

Synthesis, crystal data, structure figures, fluorescence sensing, XPS spectra, powder X-ray diffraction plots, thermogravimetric analysis, and IR. The Supporting Information is available free of charge on the ACS Publications website at DOI: 10.1021/acs.inorgchem.5b00098.

■ AUTHOR INFORMATION

Corresponding Author

* E-mail: wenlili@mail.ccnu.edu.cn.

Notes

The authors declare no competing financial interest.

■ ACKNOWLEDGMENTS

This work was financially supported by the National Nature Science Foundation of China (Grants 21171062 and 21371065).

■ REFERENCES

(1) Nolan, E. M.; Lippard, S. J. *Chem. Rev.* **2008**, *108*, 3443−3480.

(2) (a) Reynolds, M.; Stoddard, L.; Bespalov, I.; Zhitkovich, A. *Nucleic Acids Res.* **2006**, *35*, 465−476. (b) Zhitkovich, A. *Chem. Res. Toxicol.* **2005**, *18*, 3−11. (c) Levina, A.; Lay, P. A. *Coord. Chem. Rev.* **2005**, *249*, 281−298.

(3) (a) Arancibia, V.; Valderrama, M.; Silva, K.; Tapia, T. *J. Chromatogr. B: Anal. Technol. Biomed. Life Sci.* **2003**, *785*, 303−309. (b) Xiang, Y.; Mei, L.; Li, N.; Tong, A. J. *Anal. Chim. Acta* **2007**, *581*, 132−136.

(4) (a) Cui, Y. J.; Yue, Y. F.; Qian, G. D.; Chen, B. L. *Chem. Rev.* **2012**, *112*, 1126−1162. (b) Tanaka, D.; Horike, S.; Kitagawa, S.; Ohba, M.; Hasegawa, M.; Ozawa, Y.; Toriumi, K. *Chem. Commun.* **2007**, 3142−3144. (c) Xiao, Y. Q.; Cui, Y. J.; Zheng, Q.; Xiang, S. C.; Qian, G. D.; Chen, B. L. *Chem. Commun.* **2010**, *46*, 5503−5505. (d) Karmakar, A.; Manna, B.; Desai, A. V.; Joarder, B.; Ghosh, S. K. *Inorg. Chem.* **2014**, *53*, 12225. (e) Liu, D. M.; Lu, K. D.; Poon, C.; Lin, W. B. *Inorg. Chem.* **2014**, *53*, 1916−1924.

(5) (a) Lan, A. J.; Li, K. H.; Wu, H. H.; Olson, D. H.; Emge, T. J.; Ki, W.; Hong, M. C.; Li, J. *Angew. Chem., Int. Ed.* **2009**, *48*, 2334−2338. (b) Pramanik, S.; Zheng, C.; Zhang, X.; Emge, T. J.; Li, J. *J. Am. Chem. Soc.* **2011**, *133*, 4153−4155. (c) Cui, J. H.; Lu, Z. Z.; Li, Y. Z.; Guo, Z. J.; Zheng, H. G. *Chem. Commun.* **2012**, *48*, 7967−7969. (d) Zhang, S. R.; Du, D. Y.; Qin, J. S.; Bao, S. J.; Li, S. L.; He, W. W.; Lan, Y. Q.; Shen, P.; Su, Z. M. *Chem. - Eur. J.* **2014**, *20*, 3589−3594. (e) Jiang, H. L.; Tatsu, Y.; Lu, Z. H.; Xu, Q. *J. Am. Chem. Soc.* **2010**, *132*, 5586−5587. (f) Lu, Z. Z.; Zhang, R.; Li, Y. Z.; Guo, Z. J.; Zheng, H. G. *J. Am. Chem. Soc.* **2011**, *133*, 4172−4174. (g) Ma, D. X.; Li, B. Y.; Zhou, X. J.; Zhou, Q.; Liu, K.; Zeng, G.; Li, G. H.; Shi, Z.; Feng, S. H. *Chem. Commun.* **2013**, *49*, 8964−8966. (h) Gong, Y. N.; Jiang, L.; Lu, T. B. *Chem. Commun.* **2013**, *49*, 11113−11115. (i) Li, L. N.; Zhang, S. Q.; Xu, L. J.; Han, L.; Chen, Z. N.; Luo, J. H. *Inorg. Chem.* **2013**, *52*, 12323−12325. (j) Hao, Z. M.; Song, X. Z.; Zhu, M.; Meng, X.; Zhao, S. N.; Su, S. Q.; Yang, W. T.; Song, S. Y.; Zhang, H. J. *J. Mater. Chem. A* **2013**, *1*, 11043−11050.

(6) (a) Xu, F. J.; Kou, L.; Jia, J.; Hou, X. D.; Long, Z.; Wang, S. L. *Anal. Chim. Acta* **2013**, *804*, 240−245. (b) Tan, H. L.; Liu, B. X.; Chen, Y. *ACS Nano* **2012**, *6*, 10505−10511. (c) Li, X. X.; Xu, H. Y.; Kong, F. Z.; Wang, R. H. *Angew. Chem., Int. Ed.* **2013**, *52*, 13769−13733. (d) Zhou, J. M.; Shi, W.; Li, H. M.; Li, H.; Cheng, P. *J. Phys. Chem. C* **2014**, *118*, 416−426.

(7) Wen, L. L.; Zhou, L.; Zhang, B. G.; Meng, X. G.; Qu, H.; Li, D. F. *J. Mater. Chem.* **2012**, *22*, 22603−22609.

(8) Baburin, I. A.; Blatov, V. A.; Carlucci, L.; Ciani, G.; Proserpio, D. M. *J. Solid State Chem.* **2005**, *178*, 2452−2474.

(9) Chen, Y. F.; Rosenzweig, Z. *Anal. Chem.* **2002**, *74*, 5132−5138.

(10) (a) Barrio-Manso, J. L.; Calvo, P.; García, F. C.; Pablos, J. L.; Torroba, T.; García, J. M. *Polym. Chem.* **2013**, *4*, 4256−4264. (b) Zheng, M.; Xie, Z. G.; Qu, D.; Li, D.; Du, P.; Jing, X. B.; Sun, Z. C. *ACS Appl. Mater. Interfaces* **2013**, *5*, 13242−13247. (c) Xu, X. Y.; Yan, B. *ACS Appl. Mater. Interfaces* **2015**, *7*, 721−729.

(11) (a) EPA. *U.S. Drinking Water Criteria Document for Inorganic Mercury*; Environmental Criteria and Assessment Office: Cincinnati, OH, 1988. (b) Freeman, R.; Finder, T.; Willner, I. *Angew. Chem., Int. Ed.* **2009**, *48*, 7818−7821.

DOI: 10.1021/acs.inorgchem.5b00098
Inorg. Chem. 2015, 54, 7133−7135